

Dynamics of molecular alignment steered by a few-cycle terahertz laser pulse

Qi-Yuan Cheng(程起元), Yu-Zhi Song(宋玉志), Deng-Wang Li(李登旺), Zhi-Ping Liu(刘治平), and Qing-Tian Meng(孟庆田)

Citation: Chin. Phys. B, 2022, 31 (**10**): 103301. DOI: 10.1088/1674-1056/ac6eeb
Journal homepage: http://cpb.iphy.ac.cn; http://iopscience.iop.org/cpb

What follows is a list of articles you may be interested in

Direct Coulomb explosion of N_2O^{2+} induced by monochromatic extreme ultraviolet photons at 38.5 eV

Min Zhang(张敏), B Najjari, Bang Hai(海帮), Dong-Mei Zhao(赵冬梅), Jian-Ting Lei(雷建廷), Da-Pu Dong(董达谱), Shao-Feng Zhang(张少锋), Xin-Wen Ma(马新文)
Chin. Phys. B, 2020, 29 (**6**): 063302. DOI: 10.1088/1674-1056/ab8629

Field-free molecular orientation steered by combination of super-Gaussian and THz half-cycle laser pulses

Qi-Yuan Cheng(程起元), Yu-Zhi Song(宋玉志), Qing-Tian Meng(孟庆田)
Chin. Phys. B, 2019, 28 (**11**): 113301. DOI: 10.1088/1674-1056/ab4cdf

Theoretical approach to the study of vibrational effects on strong field ionization of molecules with alignment-dependent tunneling ionization rates

Zhang Mei-Xia, Yan Bing, Yang Yu-Jun, Luo Si-Zuo, Zhu Rui-Han, Yang Xue, Ding Da-Jun
Chin. Phys. B, 2015, 24 (**9**): 093302. DOI: 10.1088/1674-1056/24/9/093302

Nonsequential double ionization of diatomic molecules by elliptically polarized laser pulses

Tong Ai-Hong, Liu Dan, Feng Guo-Qiang
Chin. Phys. B, 2014, 23 (**10**): 103302. DOI: 10.1088/1674-1056/23/10/103302

Angular distributions of CH_3I fragment ions under the irradiation of single pulse and trains of ultrashort laser pulses

Song Yao-Dong, Chen Zhou, Sun Chang-Kai, Hu Zhan
Chin. Phys. B, 2013, 22 (**1**): 013302. DOI: 10.1088/1674-1056/22/1/013302

Dynamics of molecular alignment steered by a few-cycle terahertz laser pulse

Qi-Yuan Cheng(程起元)[1,2,3,4], Yu-Zhi Song(宋玉志)[2], Deng-Wang Li(李登旺)[2,3], Zhi-Ping Liu(刘治平)[4], and Qing-Tian Meng(孟庆田)[2,†]

[1] *Medical Engineering Department, Shandong Provincial Hospital Affiliated to Shandong First Medical University, Jinan* 250021, *China*
[2] *School of Physics and Electronics, Shandong Normal University, Jinan* 250358, *China*
[3] *Shandong Laibo Biotechnology Co., Ltd., Jinan* 250101, *China*
[4] *School of Control Science and Engineering, Shandong University, Jinan* 250061, *China*

(Received 3 April 2022; revised manuscript received 7 May 2022; accepted manuscript online 12 May 2022)

The field-free alignment of molecule ClCN is investigated by using a terahertz few-cycle pulse (THz FCP) based on the time-dependent density matrix theory. It is shown that a high degree of molecular alignment can be obtained by changing the matching number of the THz FCPs in the adiabatic regime and the non-adiabatic regime. The matching number can affect both the maximum value of the alignment and the time at which it is achieved. It is also found that a higher degree of alignment can be achieved by using the THz FCP at lower intensity and there exists an optimal threshold of molecular alignment with the increase of the field amplitude. Also found is the frequency sensitive region in which the degree of maximum alignment can be enhanced greatly by modulating the center frequencies of different THz FCPs. The investigation demonstrates that comparing with a THz single-cycle pulse, a better result of the field-free alignment can be created by a THz FCP at a constant rotational temperature of molecule.

Keywords: molecular alignment, few-cycle terahertz pulse, density matrix theory

PACS: 33.80.–b, 33.15.Vb, 33.80.Wz, 33.15.Kr **DOI:** 10.1088/1674-1056/ac6eeb

1. Introduction

Molecular alignment manipulated by laser pulses has been an important research topic in molecular reaction stereoscopic dynamics in recent decades.[1–4] Generally, the alignment refers to the principal axis of a molecule arranged along a laboratory-fixed axis. When a molecule is perfectly aligned, the rotational eigenstate of the molecular wave function is transformed into a pendular state after the interaction between the molecule and the laser field. Molecular alignment has a wide range of applications in various research fields, such as x-ray absorption and diffraction,[5–7] probe of the dissipative properties,[8,9] high-order harmonic generation,[10–12] and photo-association dynamics.[13–15] For a laser pulse in the terahertz (THz) region, its resonant interaction with the molecule can greatly promote the spatial effect of molecular rotation, but exert little influence on the electronic and vibrational modes of the molecule.

For decades, several intense picosecond laser pulses based on their polarization characteristics have been employed to generate the alignment through the interaction between the laser field and the molecule via permanent dipole moment and anisotropic polarizability. Normand *et al.*[16] first observed the alignment result of a thermal ensemble of CO molecules by using two linearly polarized YAG laser pulses with crossed polarizations in experiment. Then, Friedrich and Herschbach[17] theoretically proposed a mechanism to account for the alignment obtained by Normand *et al.* and showed that the molecular alignment involves hybridization strong enough to bring the eigenproperties close to the harmonic librator limit. Utilizing the non-resonant excitation, Rosca–Pruna and Vrakking[18] observed an experimental result of revival structures in the alignment of molecules by an intense laser pulse. While their schemes provided a concrete method and pointed the way of further improving the molecular alignment in the later period, the degree of molecular alignment at that time was relatively low and the adiabatic molecular alignment yielded by a relatively long pulse disappeared easily after the pulses.[19]

With the development of laser technology, many novel pulses, such as the ultrashort pulse and the shaped pulse, have been designed to improve the molecular field-free alignment under different conditions. Loriot *et al.*[20] investigated the dynamical alignment of jet-cooled OCS molecules induced nonresonantly by a short pump pulse of duration about 70 femtosecond and observed the maximum alignment under the conditions close to the saturation of ionization. Xu *et al.*[21] reported that the femtosecond laser pulse shaped with a V-style spectral phase modulation can provide a well-established scheme to control the maximum degree and temporal structure of the molecular alignment. Based on the interactions of the laser field with molecular permanent dipole, polarizability and hyperpolarizability, the field-free alignment of tri-

[†]Corresponding author. E-mail: qtmeng@sdnu.edu.cn

© 2022 Chinese Physical Society and IOP Publishing Ltd

atomic molecules were theoretically steered by shaped laser pulse with the slow turn-on and rapid turn-off (STRT) in a non-adiabatic regime.[22] However, the non-resonant short pulse laser field mainly interacts with molecules through the polarizability and hyperpolarizability, and the interaction through the permanent dipole moment is relatively weak. The molecules are exposed to intense optical irradiation prior to their interrogation, potentially producing the ionization and dissociation of molecules, which would be a severe obstacle to enhancing the molecular alignment.[23–25]

To compensate for the shortage of intense fields, it is suggested to use the terahertz (THz) pulses to control the direction of the molecular principal axis due to the strong interaction with the permanent dipole moment of molecules and small damage to the electronic and vibrational modes of molecule.[26,27] By utilizing the THz single-cycle pulses (SCPs) resonantly interacting with molecular rotations, Fleischer *et al.*[28] observed the field-free alignment of polar gas-phase molecules in a gas sample under ambient conditions. Cheng *et al.*[29] theoretically investigated the alignment of FCN molecule induced by a THz half-cycle pulse (HCP) and found a saturation threshold for molecular alignment by analyzing the 1st, 2nd, and 3rd order interactions. The orientation dynamics of several diatomic molecules under available THz few-cycle pulses (THz FCPs) was investigated through solving the time-dependent Schrödinger equation and a higher degree of orientation has been achieved at lower intensity of the laser field.[30] To further improve the molecular orientation degree, the shaped pulse followed by a THz laser pulse was designed to achieve a multi-step rotational excitation, and the result obtained became much better than that by the shaped pulse or THz laser pulse alone.[31–33]

Compared with SCP and HCP, a THz FCP has more optical cycles included in a pulse duration at the same center frequency, and it is relatively easy to generate resonance excitation and create a higher result of molecular alignment.[30] However, most of the studies using various THz pulses to steer the direction of the molecule have still concentrated on the molecular orientation over the years, and the scheme of molecular alignment induced by a THz FCP has seldom been proposed in detail by this time.[34–41] Therefore, there is a need to effectively take advantage of the THz FCP under different parameter conditions for further exploring the molecular alignment. To this end, we calculate the alignment of the molecule by using a THz FCP through solving the density matrix equation in this paper, and study the degree of molecular alignment changing with the matching number, field amplitude, central frequency and rotational temperature. The rest of this paper is arranged as follows. In Section 2, the calculation method and the model system are described. In Section 3, the simulated results and the alignment dynamics are discussed. Finally, some conclusions and perspectives are given in Section 4.

2. Description of method

Consider a linear molecule ClCN exposed to a THz FCP given by

$$E(t) = E_1(t)\cos(\omega t + \varphi) \tag{1}$$

with

$$E_1(t) = E_0 \exp\left(-2\ln 2\frac{t^2}{\tau^2}\right), \tag{2}$$

where E_0, τ, ω, and φ denote the field amplitude, the full width at half maximum (FWHM), the central frequency, and the carrier envelope phase of the THz laser pulse, respectively. The turning of τ can match the optical period $t_p = 2\pi/\omega$. Define N as the matching number, *i.e.*, the number of optical cycles contained in a pulse duration. For an SCP, $\tau = Nt_p$ ($N = 1$), and for an FCP, $\tau = Nt_p$ ($N = 2, 3, 4, \ldots$). Based on the rigid rotor approximation, the Hamiltonian of the molecule ClCN exposed to the laser field $E(t)$ can be expressed as[42]

$$\begin{aligned}\hat{H}(t) =\ & B_e\hat{J}^2 - \mu E(t)\cos\theta - \frac{1}{4}[(\alpha_\parallel - \alpha_\perp)\cos^2\theta + \alpha_\perp]E_1^2(t) \\ & - \frac{1}{8}[(\beta_\parallel - 3\beta_\perp)\cos^2\theta + 3\beta_\perp\cos\theta]E_1^2(t),\end{aligned} \tag{3}$$

where B_e is the rotational constant of the molecule, $\hat{J}$ the angular momentum operator, μ the permanent dipole moment, θ the angle between the molecular axis and the direction of the laser polarization, $\alpha_\parallel$ and $\alpha_\perp$ are the polarizability's components parallel and perpendicular to the molecular axis, respectively, $\beta_\parallel$ and $\beta_\perp$ denote the hyperpolarizabilities parallel and orthogonal to the molecular axis, respectively. In Eq. (3), the first term on the right-hand side is the molecular rotation energy and the second, third, and last terms are the potentials of interaction of the THz laser pulse with the permanent dipole moment, polarization, and hyperpolarization, respectively. The alignment degree of the molecule is given by the expectation value

$$\langle\cos^2\theta\rangle = \mathrm{Tr}\{\cos^2\theta\hat{\rho}(t)\}, \tag{4}$$

where Tr denotes the trace and $\hat{\rho}(t)$ is the time-dependent density operator. The time evolution of the density operator is determined by Liouville equation

$$\frac{\mathrm{d}\hat{\rho}(t)}{\mathrm{d}t} = -\frac{\mathrm{i}}{\hbar}[\hat{H}, \hat{\rho}(t)]. \tag{5}$$

The density operator can be expanded in the eigenstates of the rigid rotor Hamiltonian as

$$\hat{\rho}(t) = \sum_{JMJ'M'} \rho_{JMJ'M'}(t)\,|JM\rangle\langle J'M'|, \tag{6}$$

where $\rho_{JMJ'M'}(t)$ are obtained by solving the coupling differential equations[43]

$$\frac{\mathrm{d}\rho_{JMJ'M'}(t)}{\mathrm{d}t} = -\frac{\mathrm{i}}{h}\Big\{(\varepsilon_J - \varepsilon_{J'})\rho_{JMJ'M'}(t) + \mu E(t)\sum_{J_1M_1}[V^{(1)}_{J_1M_1J'M'}\rho_{JMJ_1M_1}(t) - V^{(1)}_{JMJ_1M_1}\rho_{J_1M_1J'M'}(t)]$$
$$+\frac{1}{4}\Delta\alpha E_1^2(t)\sum_{J_1M_1}[V^{(2)}_{J_1M_1J'M'}\rho_{JMJ_1M_1}(t) - V^{(2)}_{JMJ_1M_1}\rho_{J_1M_1J'M'}(t)]$$
$$+\frac{1}{8}E_1^3(t)\sum_{J_1M_1}[(\beta_{\parallel}-3\beta_{\perp})(V^{(3)}_{J_1M_1J'M'}\rho_{JMJ_1M_1}(t) - V^{(3)}_{JMJ_1M_1}\rho_{J_1M_1J'M'}(t))$$
$$+3\beta_{\perp}(V^{(1)}_{J_1M_1J'M'}\rho_{JMJ_1M_1}(t) - V^{(1)}_{JMJ_1M_1}\rho_{J_1M_1J'M'}(t))]\Big\} \quad (7)$$

with $V^{(i)}_{JMJ'M'} = \langle JM|\cos^i\theta\,|J'M'\rangle$ $(i = 1,\ 2,\ 3)$, and $\varepsilon_J = B_eJ(J+1)$. The initial density operator obeys the temperature-dependent Boltzmann distribution

$$\rho_0(T) = \frac{1}{Z}\sum_{J=0}^{\infty}\sum_{M=-J}^{M=J}|JM\rangle\langle JM|\exp\left(\frac{-B_eJ(J+1)}{k_BT}\right), \quad (8)$$

where

$$Z = \sum_{J=0}^{\infty}\sum_{M=-J}^{M=J}\exp\left(-\frac{B_eJ(J+1)}{k_BT}\right)$$

is the partition function with the Boltzmann constant k_B at temperature T.

Equation (7) is solved by using the fourth-order Runge–Kutta method, and treating ClCN as a target molecule. The ClCN is a polar molecule with a moderate permanent dipole moment of $\mu = 2.836$ D and a polarizability anisotropy of $\Delta\alpha = \alpha_{\parallel} - \alpha_{\perp} = 3.256$ Å^3.[44,45] The parallel and orthogonal hyperpolarizabilities $\beta_{\parallel} = 4.086\times10^9$ Å^5 and $\beta_{\perp} = -4.146\times10^8$ Å^5, respectively. The rotational constant $B_e = 0.199$ cm^{-1} corresponding to the rotational period $T_{\mathrm{rot}} = h/2B_e = 83.75$ ps.

3. Results and discussion

Figure 1 shows the time evolution of the molecular alignment $\langle\cos^2\theta\rangle$ steered by THz pulses at the matching number $N = 1$, 2, 3 and 4, corresponding to Figs. 1(a)–1(d), respectively. Here, the field amplitude $E_0 = 1.0\times10^7$ V/cm, central frequency $\omega = 36$ cm^{-1}, CEP $\varphi = 0$, and rotational temperature $T = 5$ K. The molecular alignment by the THz SCP with matching number $N = 1$ serves more as a proof-of-concept comparison. As can be seen, the molecular alignments by the four pulses all produce peaks during the pulse and revive regularly at $t = nT_{\mathrm{rot}}$ $(n = 0, 1, 2, \ldots)$ after the pulse, and there is a relatively strong oscillating process with an oscillation period twice as long as the rotational period of the molecule. Because the time of interaction between the laser and the molecule is much shorter than the rotational period of molecule, the process is a non-adiabatic regime. Moreover, with the matching number N increasing from 1 to 4, the duration of THz FCP becomes longer under the same center frequency, and there are two variation tendencies of the alignment: the maximum degree of in-field alignment is enhanced, and the number of oscillating peaks in post-field alignment is increased. Obviously, the number of peaks in the field-free alignment is positively correlated with the matching number of the THz pulse. The oscillation of the molecular alignment with time is possibly caused by the dispersion of the relative phases within the wave packets.[43] It is found that within a rotational period, the maximum degree of field-free alignment appears at $t = 40.35$ ps in the former oscillation under $N = 1$ and 2 pulses (Figs. 1(a) and 1(b)) and at $t = 85.41$ ps in the latter oscillation under $N = 3$ and 4 pulses (Figs. 1(c) and 1(d)). Therefore, the matching number of the THz TCP can not only suppress or enhance the maximum value of molecular alignment but also exert an important influence on the moment when the maximum value occurs.

To further explore how the matching number N affects the in-pulse and post-pulse alignment of molecule, we calculate the maximum degree of molecular alignment $\langle\cos^2\theta\rangle_{\max}$ by varying the matching number N from 1 to 20, and the result is depicted in Fig. 2. It is found that the maximum degree of molecular alignment $\langle\cos^2\theta\rangle_{\max}$ of the in-pulse and the post-pulse first increase and then decrease, and the maximum values obtained at $N = 4$ and $N = 3$ are 0.642 and 0.613, respectively. A little higher degree of $\langle\cos^2\theta\rangle_{\max}$ can be obtained after the pulse than during the pulse when the matching number $N = 1$ and 2. The maximum alignment in the field starts to be greater than after the field when $N \geq 3$, and as N continues to increase, the difference between the maximum degree of the alignment in the field and after the field also enlarges. Finally, the $\langle\cos^2\theta\rangle_{\max}$ of the in-pulse converges to a saturation value of 0.611 and the post-pulse alignment becomes weak, or even almost disappears. This may be due to the fact that with the increase of N, the duration of the pulse becomes longer and the process of molecular alignment gradually transitions from non-adiabatic to adiabatic regime, which provides a higher degree of alignment during the pulse and relatively weaker alignment after the pulse.[19] From $N = 1$ to 20, the change of maximum alignment $\Delta\langle\cos^2\theta\rangle_{\max}$ is 0.136 for the in- pulse and 0.252 for post-pulse, showing that it is easier to influence the post-pulse alignment of molecule by adjusting the matching number than by implementing the in-pulse alignment.

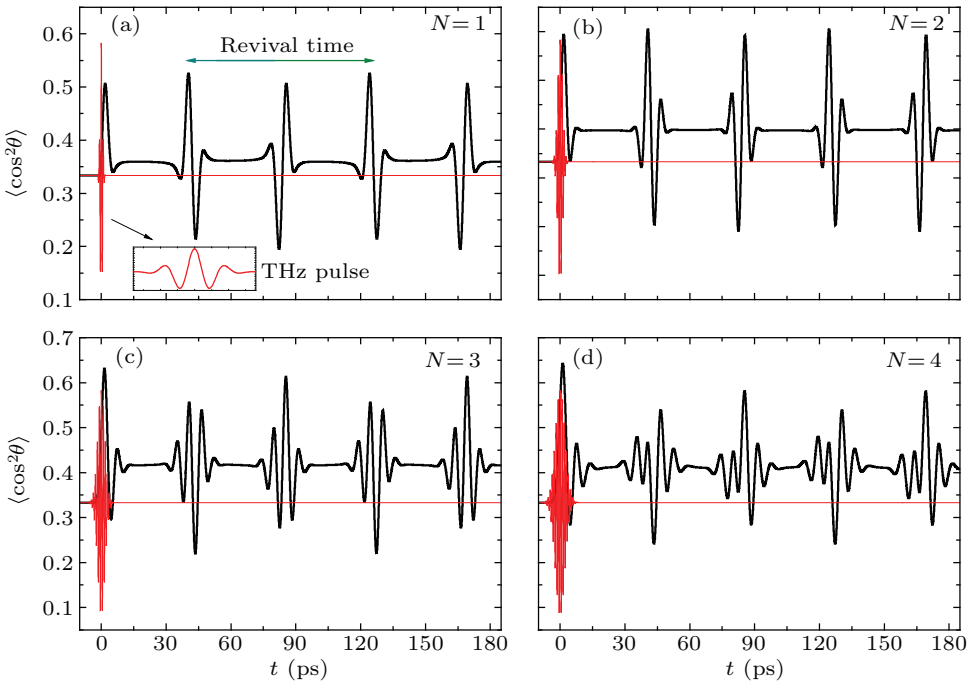


Fig. 1. Time evolution of molecular alignment by THz pulses separately for matching number $N = 1$, 2, 3 and 4, at field amplitude $E_0 = 1.0 \times 10^7$ V/cm, central frequency $\omega = 36$ cm^{-1}, CEP $\varphi = 0$, and rotational temperature $T = 5$ K.

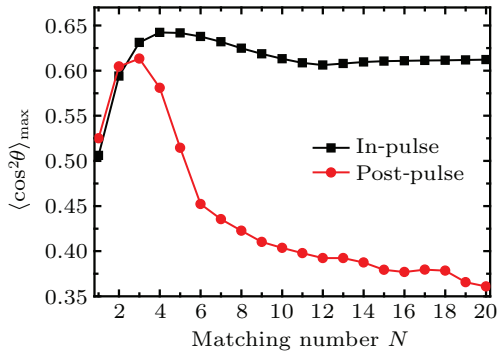


Fig. 2. Maximum degree of molecular alignment $\langle\cos^2\theta\rangle_{\max}$ at rotational temperature $T = 5$ K *versus* matching number N of THz FCP for field amplitude $E_0 = 1.0 \times 10^7$ V/cm, central frequency $\omega = 36$ cm^{-1}, and CEP $\varphi = 0$.

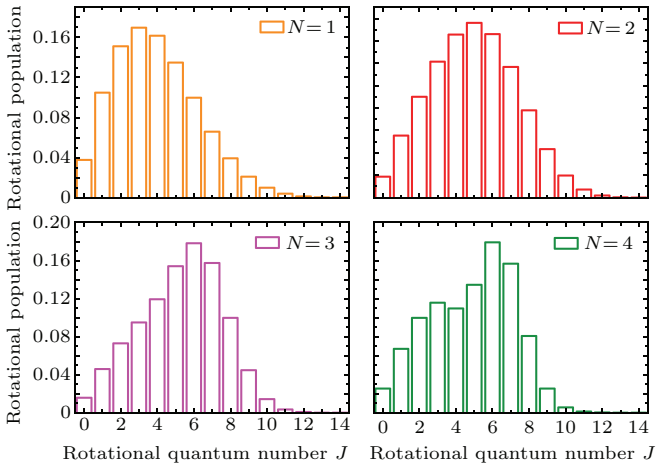


Fig. 3. Rotational population at matching number $N = 1$, 2, 3, and 4 of THz pulses. The other parameters are same as in Fig. 2.

To elucidate the physical mechanism of molecular alignment influenced by different THz FCPs, we further study the population of field-free molecular alignment in each rotational quantum state. Figure 3 shows the rotational population for the matching number $N = 1$ (orange column), 2 (red column), 3 (magenta column), and 4 (olive column) of the THz pulses in sequence with the field amplitude $E_0 = 1.0 \times 10^7$ V/cm, the central frequency $\omega = 36$ cm^{-1}, and the CEP $\varphi = 0$. It can be found that the rotational population remains in quantum states $J \leq 12$ with N changing from 1 to 4 and the maximal values of rotational population appear at $J = 3$, 5, 6, and 6 respectively. Comparing with the THz SCP ($N = 1$), the population induced by the THz FCPs obviously decreases in low rotational states ($J \leq 4$), but greatly increases in high rotational states ($J > 4$). The phenomenon reflects that the THz FCP is easier to promote the population in the higher rotational state.

Obtaining the post-pulse alignment as high as possible is critical for practical applications of the aligned molecules. To find out the optimal value of $\langle\cos^2\theta\rangle_{\max}$ after the pulse, the electric field amplitude E_0 changes from 1 MV/cm to 17 MV/cm separately at the matching number $N = 1$ and 3. It is shown in Fig. 4 that black squares represent the maximum alignment under $N = 1$ pulse and red circles denote the maximum alignment under $N = 3$ pulse. It can be seen that with the increase of the electric field amplitude E_0, the maximum alignment $\langle\cos^2\theta\rangle_{\max}$ first increases from 0.341 to 0.638 for $N = 1$ pulse and from 0.337 to 0.643 for $N = 3$ pulse. The peak values of maximum alignment can be obtained when the field amplitude $E_0 = 12$ MV/cm and 14.5 MV/cm. Compared with using the $N = 1$ pulse, using the $N = 3$ pulse can achieve a higher degree of molecular alignment when the field amplitude is relatively small. As the electric field amplitude E_0 continues to increase, the maximum alignment $\langle\cos^2\theta\rangle_{\max}$ be-

gins to decrease, and the nonlinear effect appears obviously. In this case, the increase of the laser intensity will restrain the improvement of molecular alignment. Although the central frequency used in our simulation remains unchanged, the nonlinear effect, such as alternating current (ac) Stark effect induced by an intense THz FCP, can shift the rotational population of ClCN molecule from high quantum level to low one. It is found that the alignment degree decreases more obviously by $N = 3$ pulse than by $N = 1$ pulse. It is demonstrated that the THz FCP has an advantage in improving the degree of field-free alignment with respect to the THz SCP within a specific laser intensity range, *i.e.* the electric field amplitude $E_0 \leq 13$ MV/cm. Obviously, there exists an optimal threshold for molecular alignment implemented by the THz FCP, and the matching number has a certain influence on the position of alignment peak. At this time, the rotational population of the molecule is the positively skewed normal distribution, and the distribution will be destroyed when the laser intensity exceeds the saturation threshold which leads the maximum alignment degree to decrease.[29]

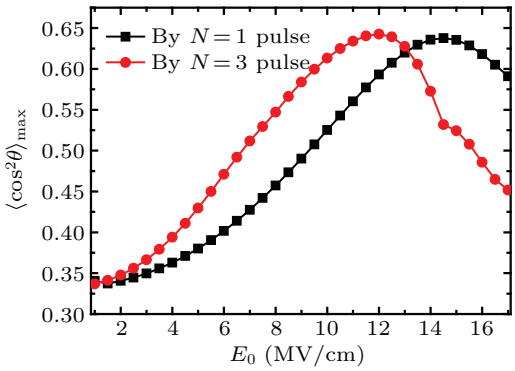


Fig. 4. Maximum degree of molecular alignment $\langle\cos^2\theta\rangle_{\max}$ *versus* field amplitude E_0 of THz FCP at matching number $N = 1$ and 3, respectively.

For a THz FCP, the change of center frequency must have a great influence on the alignment dynamics of the molecule. Figure 5 depicts the maximum degree of molecular alignment $\langle\cos^2\theta\rangle_{\max}$ induced by the matching number $N = 1$ (black squares), 2 (red circles), 3 (blue uptriangles), and 4 (magenta downtriangles) pulses at the rotational temperature $T = 5$ K as a function of central frequency ω for the CEP $\varphi = 0$ and the field amplitude $E_0 = 12$ MV/cm, respectively. With the central frequency of a THz FCP increasing from 25 cm^{-1} to 200 cm^{-1}, the maximum degrees of all alignments first increase rapidly and then decrease gradually. The peak values appear at the central frequency $\omega = 31$, 34, 36, and 42 cm^{-1} corresponding to 0.626, 0.654, 0.642, and 0.583, respectively. It can be seen that the alignment peaks shift from lower to higher frequency when the matching number increases from $N = 1$ to 4. With the matching number $N = 2$, an optimal molecular alignment induced by a THz FCP is obtained at the central frequency of about 34 cm^{-1}, corresponding to 1.02 THz. Next, by defining the frequency width at nine-tenths of peak value as the bandwidth $\Delta\omega$ of the THz FCP, we can find that the sensitive regions of molecular alignment under $N = 1$, 2, 3, and 4 pulses are about 26 cm^{-1}–42 cm^{-1}, 30 cm^{-1}–48 cm^{-1}, 31 cm^{-1}–52 cm^{-1}, and 28 cm^{-1}–80 cm^{-1}, corresponding to the bandwidth $\Delta\omega = 16$, 18, 21, and 52 cm^{-1} respectively. The degree of molecular alignment can be obviously enhanced within those frequency ranges. This is due to the fact that the molecule can absorb more energy from those frequency ranges, and higher rotational energy levels of the molecule can be populated. This result suggests that an appropriate design of the center frequency specific to different THz FCPs is required to achieve a superior degree of field-free molecular alignment.

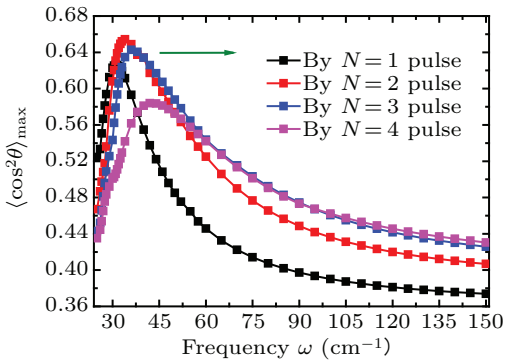


Fig. 5. Curves of maximum degree of molecular alignment $\langle\cos^2\theta\rangle_{\max}$ at the rotational temperature $T = 5$ K *versus* central frequency ω of THz FCP with CEP $\varphi = 0$ and field amplitude $E_0 = 12$ MV/cm, respectively, for $N = 1$–4.

The above simulations are performed by only changing laser pulse parameters at constant rotational temperature. According to the temperature-dependent Boltzmann distribution, more rotational states can be populated with the increase of temperature. We further regulate the molecular rotational temperature to investigate the alignment features by the THz FCP, with other conditions unchanged. The time evolution of molecular alignment and the population of rotational state at the temperature $T = 5$, 10, and 15 K are given in Fig. 6. It is found from Fig. 6(a) that the rotational temperature can only affect the peak values of the molecular alignment revivals after turn-off of the pulse, and the degrees of maximum alignment are 0.654, 0.556, and 0.489, respectively. The durations of peaks are 2.90, 2.56, and 2.23 ps, when the alignment degree $\langle\cos^2\theta\rangle > 0.4$, corresponding to the temperature $T = 5$, 10, and 15 K respectively. During those durations, the electron dynamic behaviors of these angular distributions can easily be probed by using femtosecond or picosecond laser pulses in practical application.[46] Figure 6(b) illustrates the populations of the rotational quantum states at different temperatures. Apparently, the molecules mainly populate on the quantum states

of $J \leq 16$ and the maximum values of population are obtained when the rotational quantum number $J = 8$, corresponding to 0.154, 0.134 and 0.121 respectively. As the temperature T increases from 5 K to 15 K, the rotational population of molecules gradually shifts from lower to higher quantum energy level. This result is a reversal process of the population transfer induced by changing the laser parameters or adding another pulse, where the alignment can be improved when the rotational population is shifted from lower to higher quantum state. Since the rate of angular dephasing increases with the number of rotational states increasing, the degree of molecular alignment decreases with temperature increasing.[34]

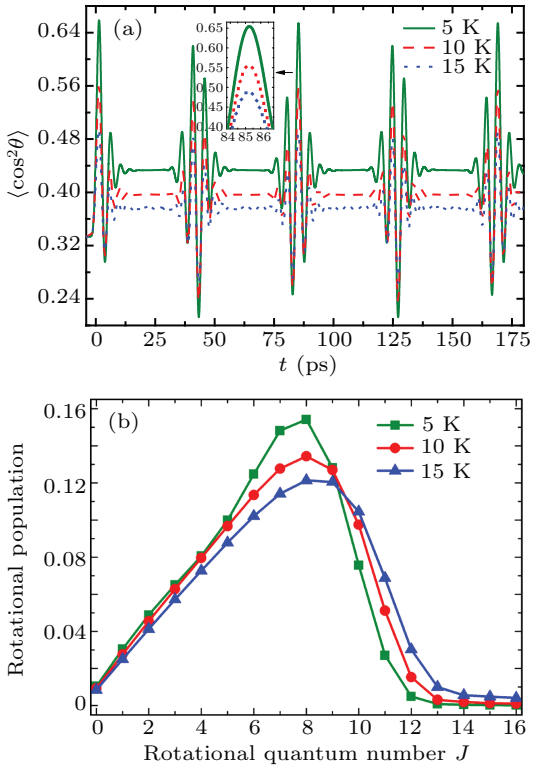


Fig. 6. Plots of (a) alignment *versus* time and (b) population of rotational states *versus* rotational quantum number at molecular temperature $T = 5$ K (olive line), 10 K (red line), and 15 (blue line), for field amplitude $E_0 = 120$ MV/cm, CEP $\varphi = 0$, and matching number $N = 2$.

4. Conclusions

Based on a quantum mechanical calculation, we have investigated the ClCN molecular alignment steered by the THz FCP. Our results show that the maximum degree of molecular alignment is closely related to the laser parameters including the matching number, field amplitude, and central frequency. The matching number can not only enhance the maximum degree of the alignment but also have a crucial influence on the moment of the maximum value. The molecular alignment in both non-adiabatic regime and the adiabatic regime can effectively be achieved when the matching number is adjusted appropriately. Moreover, the THz FCP has an advantage in improving the degree of field-free alignment with respect to the THz SCP with a given laser intensity. For different THz FCPs, there are different frequency bandwidths within which the maximum alignment can be greatly enhanced and the bandwidth moves towards high frequency with the increase of the matching number. The rotational temperature can affect only the peak values of the molecular alignment revivals and a high molecular alignment can be realized at a low temperature. Since the duration of field-free alignment peak by the appropriate design of THz FCP can be long enough, we believe that the technique will have important applications in ultrafast optical detection and other related fields. Certainly the above conclusions need further supporting from experimental evidence.

Acknowledgements

Project supported by the National Natural Science Foundation of China (Grant Nos. 12274265 and 11874241) and the Taishan Scholar Project of Shandong Province, China.

References

[1] Zeng G P, Zhong F J, Wu C Y, Jiang H B and Gong Q H 2009 *Laser Phys.* **19** 1691
[2] Leibscher M, Averbukh I S and Rabitz H 2003 *Phys. Rev. Lett.* **90** 213001
[3] Chatterley A S, Schouder C, Christiansen L, Shepperson B, Rasmussen M H and Stapelfeldt H 2019 *Nat. Commun.* **10** 133
[4] Floß J and Brumer P 2017 *J. Chem. Phys.* **146** 124313
[5] Ospelkaus S, Ni K K, Wang D, Miranda M H G, Neyenhuis B, Quéméner G, Julienne P S, Bohn J L, Jin D S and Ye J 2010 *Science* **327** 853
[6] Spence J C H, Schmidt K, Wu J S, Hembree G, Weierstall U, Doak B and Fromme P 2005 *Acta Crystallogr. Sect. A* **61** 237
[7] Peterson E R, Buth C, Arms D A, Dunford R W, Kanter E P, Krassig B, Landahl E C, Pratt S T, Santra R, Southworth S H and Young L 2008 *Appl. Phys. Lett.* **92** 094106
[8] Ramakrishna S and Seideman T 2005 *Phys. Rev. Lett.* **95** 113001
[9] Ramakrishna S and Seideman T 2006 *J. Chem. Phys.* **124** 034101
[10] Kanai T, Minemoto S and Sakai H 2007 *Phys. Rev. Lett.* **98** 053002
[11] Bian X B and Bandrauk A D 2012 *Phys. Rev. A* **86** 053417
[12] Guo X L, Jin C, He Z Q, Zhao S F, Zhou X X and Cheng Y 2021 *Chin. Phys. Lett.* **38** 123301
[13] Hu J W and Han Y C 2021 *J. Chem. Phys.* **155** 064108
[14] Kallush S, Carini J L, Gould P L and Kosloff R 2017 *Phys. Rev. A* **96** 053613
[15] Wang B B, Han Y C and Cong S L 2015 *J. Chem. Phys.* **143** 094303
[16] Normand D, Lompré L A and Cornaggia C 1992 *J. Phy. B: At. Mol. Opt. Phys.* **25** L497
[17] Friedrich B and Herschbach D 1995 *Phys. Rev. Lett.* **74** 4623
[18] Rosca-Pruna F and Vrakking M J J 2001 *Phys. Rev. Lett.* **87** 153902
[19] Torres R, Nalda R de and Marangos J P 2005 *Phys. Rev. A* **72** 023420
[20] Loriot V, Tzallas P, Benis E P, Hertz E, Lavorel B, Charalambidis D and Faucher O 2007 *J. Phys. B: At. Mol. Opt. Phys.* **40** 2503
[21] Xu S, Yao Y, Lu C, Ding J, Jia T, Zhang S Aand Sun Z 2014 *Phys. Rev. A* **89** 053420
[22] Cheng Q Y, Song Y Z and Meng Q T 2021 *Mol. Phys.* **119** e1859147
[23] Muramatsu M, Hita M, Minemoto S and Sakai H 2009 *Phys. Rev. A* **79** 011403
[24] Zhang S A, Shi J, Zhang H, Jia T, Wang Z and Sun Z R 2011 *Phys. Rev. A* **83** 023416
[25] Hu S L, Zhao Z X and Shi T Y 2013 *Chin. Phys. Lett.* **30** 103103
[26] Qin C C, Tang Y, Wang Y M and Zhang B 2012 *Phys. Rev. A* **85** 053415
[27] Matos-Abiague A and Berakdar J 2003 *Phys. Rev. A* **68** 063411

[28] Fleischer S, Zhou Y, Field R W and Nelson K A 2011 *Phys. Rev. Lett.* **107** 163603
[29] Cheng Q Y, Liu J S, Zhou X C, Song Y Z and Meng Q T 2019 *Europhys. Lett.* **125** 33001
[30] Shu C C, Yuan K J, Hu W H and Cong S L 2010 *J. Chem. Phys.* **132** 244311
[31] Liu Y, Li J, Yu J and Cong S L 2013 *Laser Phys. Lett.* **10** 076001
[32] Sonoda K, Iwasaki A, Yamanouchi K and Hasegawa H 2018 *Chem. Phys. Lett.* **693** 114
[33] Liu J S, Cheng Q Y, Yue D G, Zhou X C and Meng Q T 2018 *Chin. Phys. B* **27** 033301
[34] Machholm M and Henriksen N E 2001 *Phys. Rev. Lett.* **87** 193001
[35] Dion C M, Keller A and Atabek O 2001 *Eur. Phys. J. D* **14** 249
[36] Zhang X M, Li J, Yu J and Cong S L 2016 *Commun. Comput. Phys.* **20** 689
[37] Shu C C and Henriksen N E 2013 *Phys. Rev. A* **87** 013408
[38] Kitano K, Ishii N, Kanda N, Matsumoto Y, Kanai T, Kuwata-Gonokami M and Itatani J 2013 *Phys. Rev. A* **88** 061405
[39] You D and Bucksbaum P H 1997 *J. Opt. Soc. Am. B* **14** 1651
[40] Kitano K, Ishii N and Itatani J 2011 *Phys. Rev. A* **84** 053408
[41] Qin C C, Liu Y Z, Zhang X Z and Liu Y F 2013 *Chin. Phys. Lett.* **30** 023301
[42] Dang H P, Wang S, Zhan W S, Zai J B and Han X 2015 *Chem. Phys.* **461** 81
[43] Cheng Q Y, Liu J S, Zhou X C, Yue D G and Meng Q T 2018 *J. Phys. B: At. Mol. Opt. Phys.* **51** 065401
[44] Maroulis G and Pouchan C 1997 *Chem. Phys.* **215** 67
[45] Lafferty W J and Lide D R 1967 *J. Mol. Spectrosc.* **23** 94
[46] Sugny D, Keller A, Atabek O, Daems D, Dion C M, Guérin S and Jauslin H R 2004 *Phys. Rev. A* **69** 033402